



AMS
American Meteorological Society

Supplemental Material

© Copyright 2021 [American Meteorological Society](https://www.ametsoc.org) (AMS)

For permission to reuse any portion of this work, please contact permissions@ametsoc.org. Any use of material in this work that is determined to be “fair use” under Section 107 of the U.S. Copyright Act (17 USC §107) or that satisfies the conditions specified in Section 108 of the U.S. Copyright Act (17 USC §108) does not require AMS’s permission. Republication, systematic reproduction, posting in electronic form, such as on a website or in a searchable database, or other uses of this material, except as exempted by the above statement, requires written permission or a license from AMS. All AMS journals and monograph publications are registered with the Copyright Clearance Center (<https://www.copyright.com>). Additional details are provided in the AMS Copyright Policy statement, available on the AMS website (<https://www.ametsoc.org/PUBSCopyrightPolicy>).

Supplemental material for
The role of the Maritime Continent SST anomalies in maintaining the
Pacific–Japan pattern on decadal time scales

Mingmei Xie^{1,2}, Chunzai Wang^{1,3,4*}, Sheng Chen^{1,3,4}

¹ State Key Laboratory of Tropical Oceanography, South China Sea Institute of Oceanology,
Chinese Academy of Sciences, Guangzhou, China.

² University of Chinese Academy of Sciences, Beijing, China.

³ Southern Marine Science and Engineering Guangdong Laboratory (Guangzhou), Guangzhou,
China.

⁴ Innovation Academy of South China Sea Ecology and Environmental Engineering, Chinese
Academy of Sciences, Guangzhou, China.

Revised to *Journal of Climate*

October 2021

*Corresponding author address: Dr. Chunzai Wang, State Key Laboratory of Tropical
Oceanography, South China Sea Institute of Oceanology, Chinese Academy of Sciences,
Guangzhou, China.

Email: cwang@scsio.ac.cn

Figures

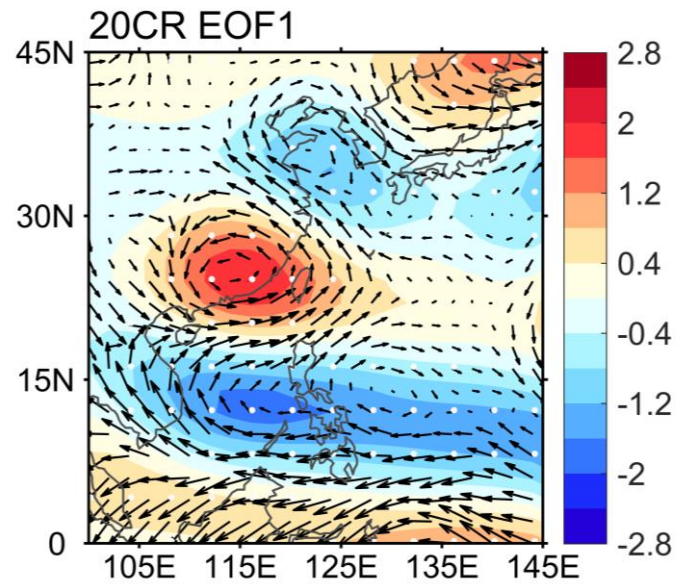


Fig. S1. The leading mode (EOF1) of JJA 850-hPa wind anomalies over the whole East Asia (0° – 45° N, 100° – 145° E) for the period of 1900-2012 from 20CR, in which the variability lower than 7 years has been removed. Shading implies relative vorticity anomalies (shading, 10^{-6} s^{-1}) regressed upon the corresponding standardized PC time series. White dots denote anomalies significant at the 90% confidence level.

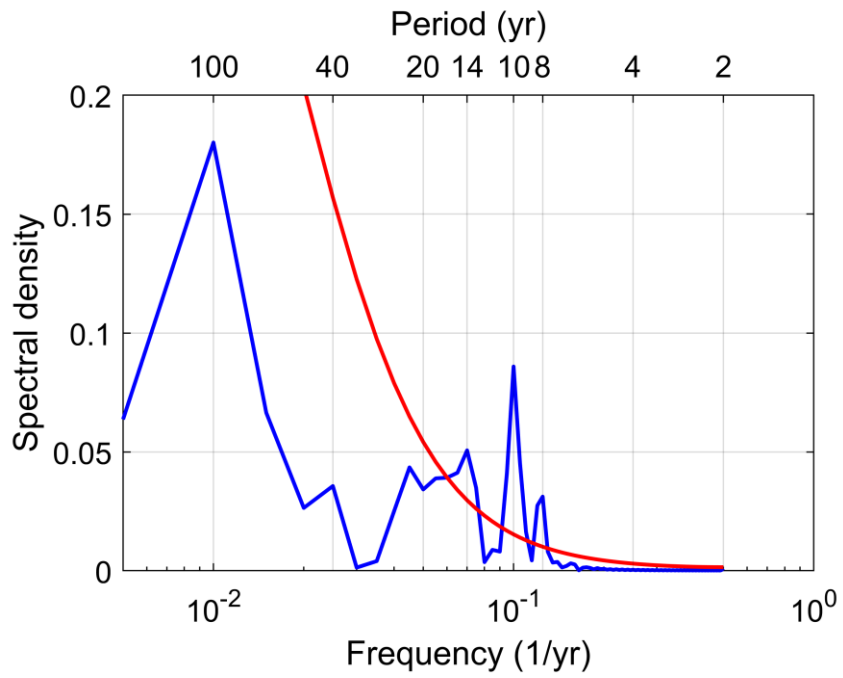


Fig. S2. The power spectrum of the MC SST index. The red curve denotes the 95% confidence limit from the red-noise estimation.

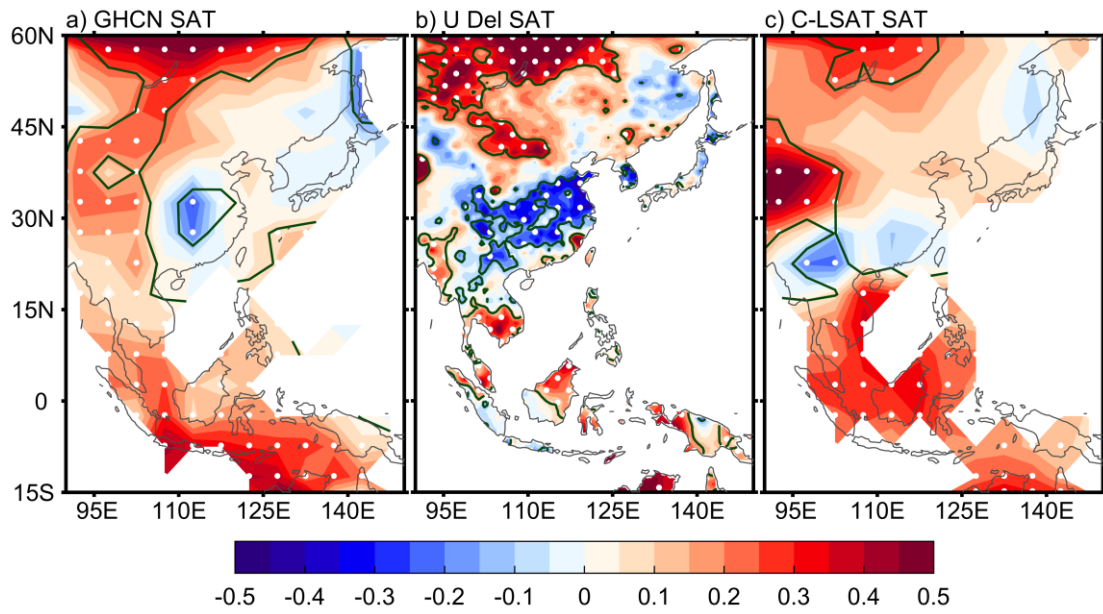


Fig. S3. Composites of JJA SAT anomalies (shading, °C) from (a) GHCN, (b) U Del and (c) C-LSAT. The regions stippled by white dots and encompassed by green lines denote where the values are significant at the 90% confidence level. The composites show the differences for positive minus negative phases of the MC SST index in Fig. 2b.

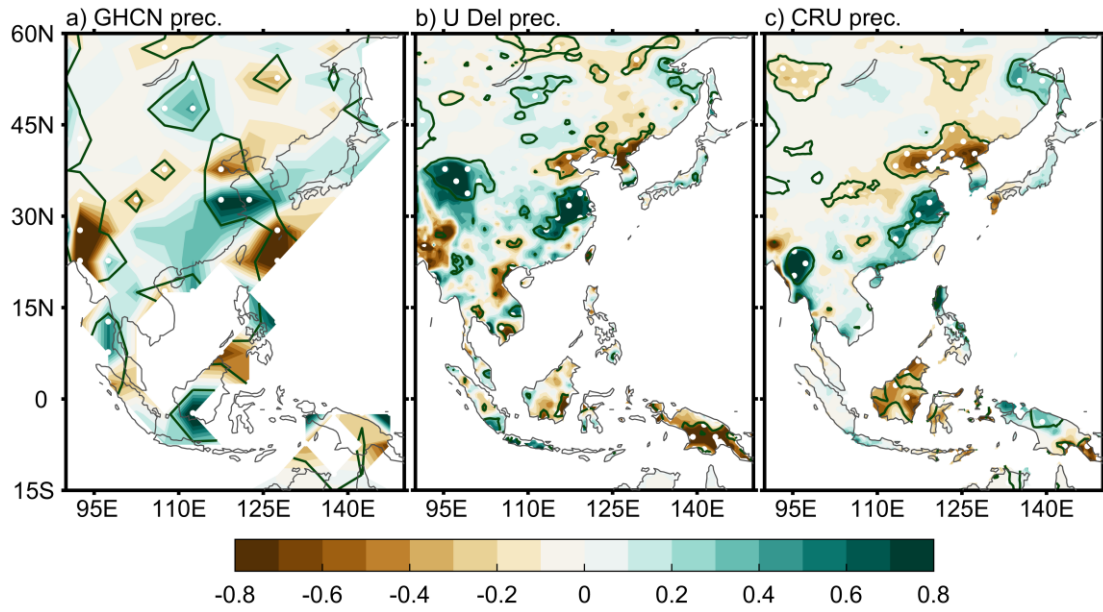


Fig. S4. Composites of JJA precipitation anomalies (shading, mm day⁻¹) from (a) GHCN, (b) U Del and (c) CRU. The regions stippled by white dots and encompassed by green lines denote where the values are significant at the 90% confidence level. The composites show the differences for positive minus negative phases of the MC SST index in Fig. 2b.

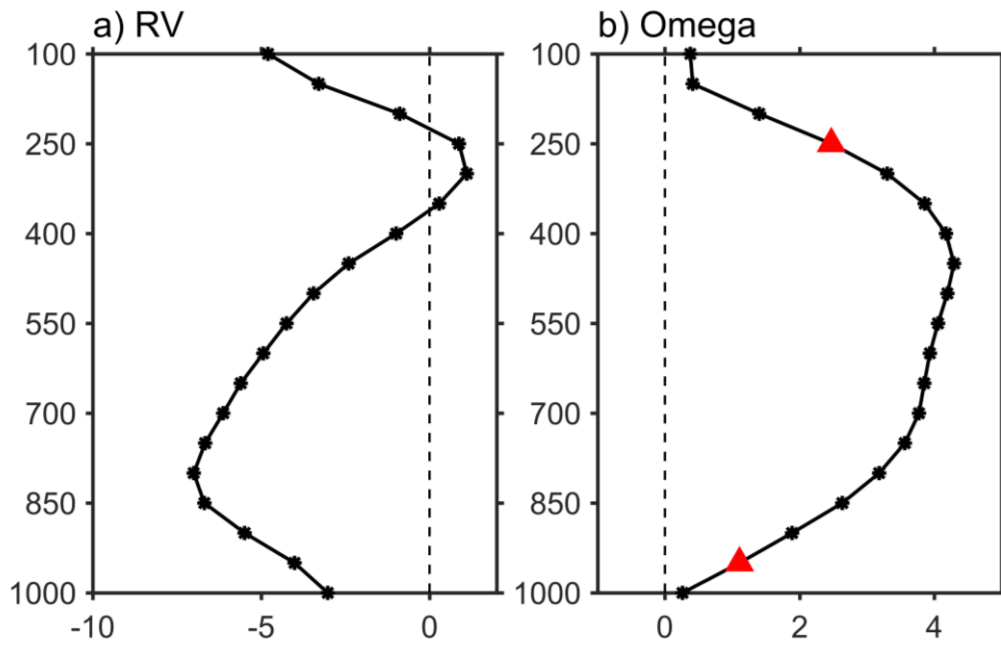


Fig. S5. Vertical profiles of regressed (a) relative vorticity (10^{-7} s^{-1}) and (b) vertical velocity ($10^{-3} \text{ Pa s}^{-1}$) over the centers of anomalous anticyclone and subsidence, respectively. The red triangles represent the maximum/minimum gradient.

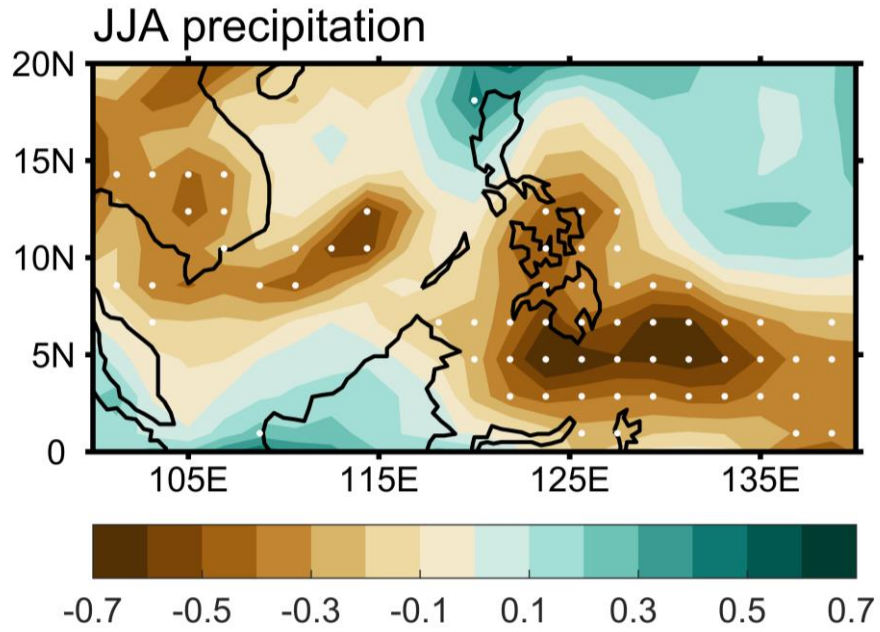


Fig. S6. Regression map of the SCS summer precipitation anomalies (shading, mm day^{-1}) onto the standardized MC SST index. White dots denote precipitation anomalies significant at the 90% confidence level.

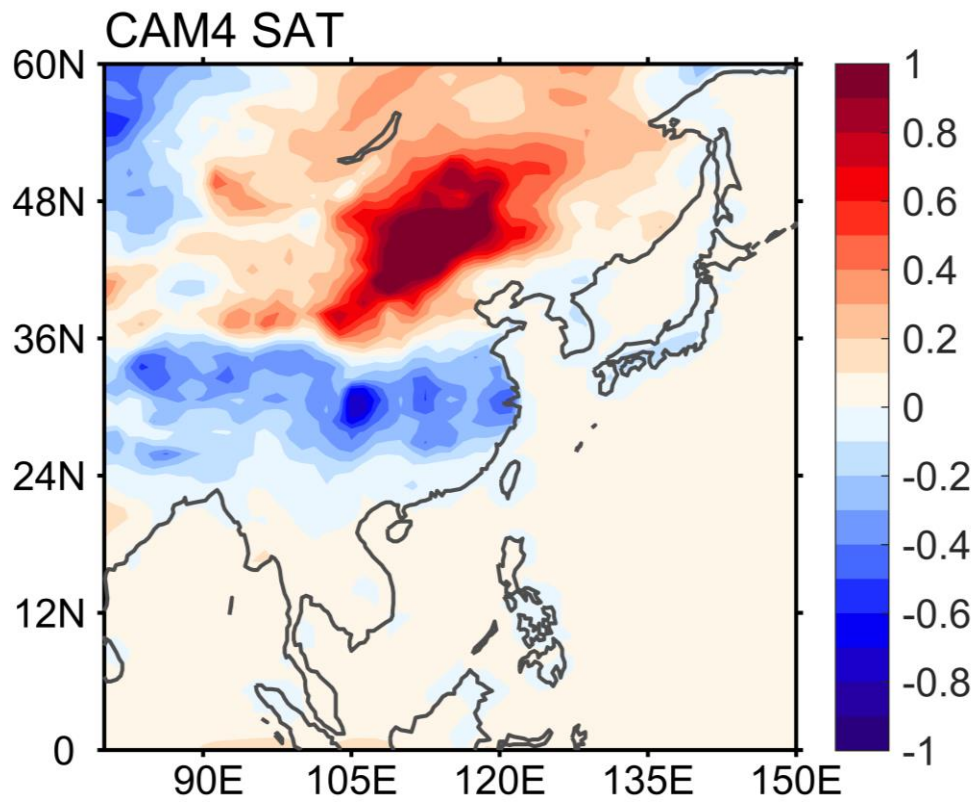


Fig. S7. The JJA mean SAT (shading, °C) differences between the MC run and the control run.

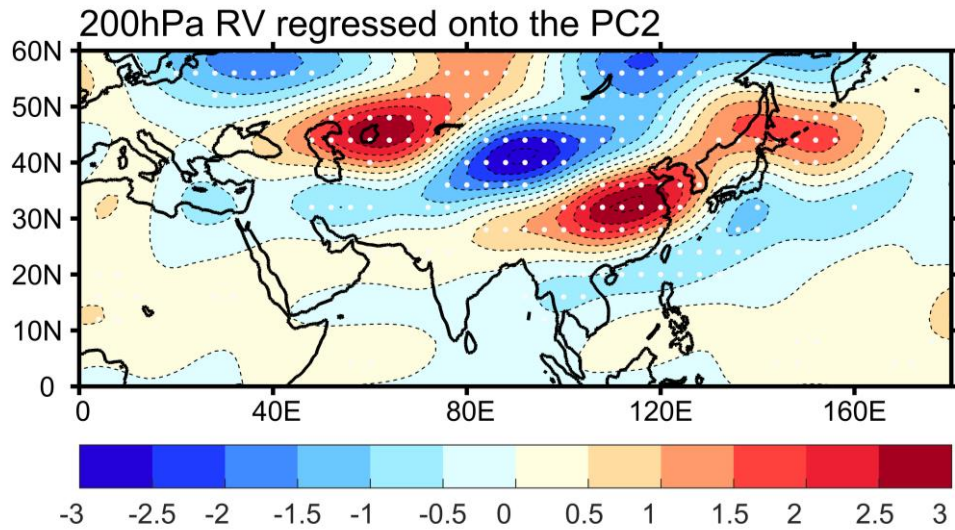


Fig. S8. Summer 200-hPa vorticity anomalies (shading, 10^{-6} s^{-1}) regressed onto the standardized PC time series of the second EOF mode, which is derived from the decadal variations of 200-hPa vorticity over the 30° – 40° N, 80° – 120° E.